

Magnetic properties of 3d transition metal wires on vicinal Cu(111) surfaces at finite temperature

H. Hashemi,^{1,a)} G. Fischer,¹ W. Hergert,¹ and V. S. Stepanyuk²

¹Institut für Physik, Martin-Luther-Universität, Halle-Wittenberg, Von-Seckendorff-Platz 1, D-06120 Halle, Germany

²Max-Planck-Institut für Mikrostrukturphysik, Weinberg 2, D-06120 Halle, Germany

(Presented 21 January 2010; received 31 October 2009; accepted 11 January 2010; published online 5 May 2010)

One-dimensional transition metal (TM) nanowires can be formed on a stepped Cu(111) surface. The basic template is an embedded Fe chain at one-atom distance away from the upper edge of the monoatomic surface step, supplying the deposition of 3d TM chains from V to Co to form on top of the Fe chain. Density functional theory (DFT) is applied to calculate the magnetic properties of these TM-Fe wires. Exchange parameters are extracted from the DFT calculations. A classical Heisenberg model is used in Monte Carlo simulations to study finite temperature effects. © 2010 American Institute of Physics. [doi:10.1063/1.3368794]

I. INTRODUCTION

Magnetic nanostructures on surfaces are of great interest for modern nanoscience due to their potential application as atomic-scale magnetic devices.^{1,2} Therefore, nanoscale clusters, monoatomic wires, or quasi-one-dimensional stripes have been investigated from experimental^{3–8} and theoretical points of view.^{9–16} The lower coordination of the magnetic atoms in such systems located on a metallic surface compared to bulk leads to an enhancement of the moments, and a large magnetocrystalline anisotropy energy (MAE) can help to stabilize the direction of the magnetic moments. The Cu(111) stepped surface with an embedded Fe chain can be considered as an exemplary template for the deposition of other 3d transition metal (TM) atoms to form a chain on top of this embedded Fe chain (cf. Fig. 1). The growth mechanism of such templates was investigated by Guo *et al.*⁵ and Mo *et al.*⁸ by means of DFT calculations and by scanning tunnelling microscopy. To use a clear notation, a single linear periodic arrangement of atoms will be called a chain in the following investigation, while a system consisting of two parallel chains, either isolated or embedded in the Cu(111) surface, will be named wire.

We will focus our discussion on the magnetic properties of the wires. Detailed information on the real structure of such systems is given elsewhere.¹⁷ We present a systematic investigation of the magnetic ground states and the magnetic coupling in TM-Fe wires. The analysis of the exchange coupling and of the MAE allows to set up a classical Heisenberg model to study finite temperature effects.

II. COMPUTATIONAL DETAILS

The calculations are performed within the framework of spin-polarized density functional theory using the Vienna *ab initio* simulation package.^{18,19} The frozen-core full-potential projector augmented-wave method (PAW) is used²⁰ applying

the generalized gradient approximation of Perdew and Wang (PW91-GGA).²¹ Computational details and convergence checks are the same as those in Ref. 17 and 22. The isolated chains and wires are modeled as a two-dimensional array of infinitely long units, keeping the distance to be at least 13 Å. A large plane-wave cutoff energy of 350 eV is used for all 3d TM chains. 25 k-points are used to sample the one-dimensional Brillouin zone. A supercell containing six Cu layers, which corresponds to 60 Cu atoms, is constructed to model the Cu(111) stepped surface (cf. Fig. 1). The same construction was used by Mo *et al.*¹⁴

For the Monte Carlo (MC) simulations, lattices of the size of 5200 sites representing the atoms of the single wire are used. Nearest-neighbor exchange interaction is assumed to define the classical Heisenberg Hamiltonian $H = -\sum_{\langle i,j \rangle} J_{ij} \vec{e}_i \cdot \vec{e}_j - \sum_i \Delta e_{i,z}^2$, where $\langle i,j \rangle$ denotes summation over pairs of classical unit spinvectors $\vec{e}_{i,j}$ interacting via J_{ij} . Anisotropy effects are taken into account by taking the MAE Δ to be 0, 0.01, 0.03, 0.10, 0.30, 1, 3, or 9 meV per site. By doing so, it is assumed that the MAE of Fe and the TM sublattices are equal. Periodic boundary conditions in direction of the wire are applied. To find the critical temperature

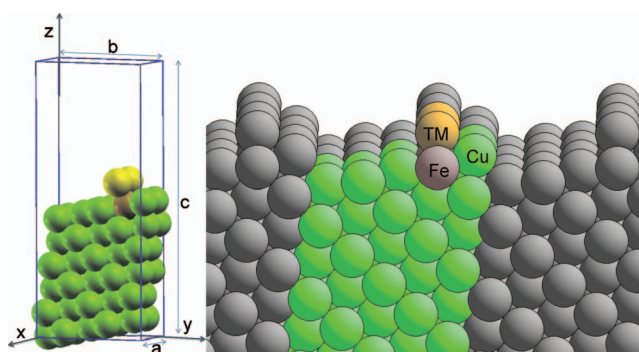


FIG. 1. (Color) TM-Fe wires on vicinal Cu(111) surface. A one-atom wide TM chain (yellow) is formed on top of an embedded Fe chain (red). Dimensions of the supercell: $a=5.14$ Å, $b=10.59$ Å, and $c=25.69$ Å. (Colored atoms in the structure on the right hand side represent the unit cell.)

^{a)}Electronic mail: hossein.hashemi@physik.uni-halle.de.

(T_C), the system is first relaxed into thermodynamical equilibrium using 20 000 MC steps per temperature step. Then, averaging is done over 30 000 measurements, between each of which three MC steps are performed in order to reduce correlation effects. To improve the statistics, averaging over at least ten of such temperature loops is performed. Importance sampling is done using the Metropolis algorithm. The T_C 's are determined using the specific heat and, in case of a ferromagnetic system, the susceptibility χ and fourth-order cumulant U_4 .

III. DISCUSSION

Three systems are investigated. In freestanding TM chains, the atomic distance is constrained to the Cu bond length d_{Cu} of the Cu(111) substrate in order to simulate a freestanding equivalent to the TM chain in the TM-Fe wire on the substrate. A freestanding wire is studied as an equivalent to the one embedded into the Cu(111) surface (cf. Fig. 1). All interatomic distances correspond to the Cu bond length of the substrate in this case. The structure of the embedded TM-Fe wire is fully relaxed. The main effect of structural relaxations is an inward relaxation of the TM atoms relative to their ideal positions. For Mn-Fe, the inward relaxation of Mn is 16% (related to Cu lattice plane distance). The Fe chain also shows an inward relaxation of 7%, respectively. Details of the relaxations for all 3d TM-Fe wires are given in Ref. 17.

Central task for the mapping onto a classical Heisenberg model is the determination of exchange constants and the MAE. The former can, for example, be extracted from DFT calculations either by the comparison of total energies of several artificial collinear magnetic structures or by applying the magnetic force theorem in the framework of the Korrinaga-Kohn-Rostoker Green's function method.^{23,24} In this work, artificial noncollinear structures are used. The idea is to choose such noncollinear states that exchange interactions in the Heisenberg model can be switched on or off in a controlled manner. Investigations of the freestanding TM chains by means of total energy considerations and magnetic force theorem reveal that the nearest neighbor exchange interaction is the most important one. The next-nearest neighbor interaction is already an order of magnitude smaller. Therefore, we restrict the Heisenberg model to nearest neighbor interactions only. Noncollinear configurations used to calculate the exchange parameters for freestanding and embedded wires are given in Fig. 2. It is checked that the magnetic moments are constant for the different noncollinear configurations used for a specific system. Noncollinear arrangements being equivalent by symmetry lead to the same exchange parameters. The exchange parameters for all systems calculated by such a procedure are given in Table I. The discussion is restricted to the TM elements from V to Co because it is not possible to stabilize all necessary magnetic configurations for the other elements. In Ref. 17, the magnetic groundstates of such freestanding and embedded wires were investigated for ideal structures by means of collinear spin-polarized DFT calculations. The magnetic groundstates for the free chains are in agreement with the results of Tung

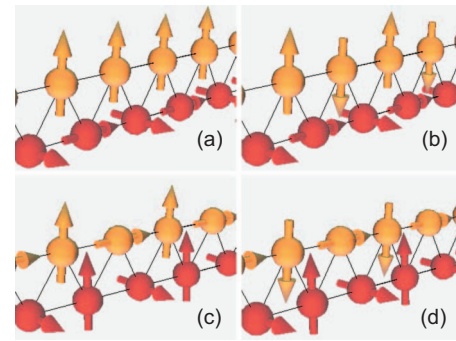


FIG. 2. (Color) Noncollinear arrangement of spin moments to determine exchange constants. [(a) and (b)] The spins moments at the Fe atoms (red) are oriented such that nearest-neighbor interactions in-between the Fe chain and between Fe and TM chain (yellow) cancel out in the Heisenberg Hamiltonian. $J_{\text{TM-TM}}$ can be calculated. [(c) and (d)] Configurations that allow to calculate the interaction $J_{\text{TM-Fe}}$ between the chains.

and Guo¹¹ for the relaxed chains with V as an exception. This can be understood easily because the relaxed bond length in the ferromagnetic state is close to the Cu bond length, whereas in the antiferromagnetic ground state the bond length is 20.2% smaller than d_{Cu} . The exchange constants reflect the antiferromagnetic groundstates of Cr and Mn chains. Noncollinear calculations for such 3d-TM chains reveal that the easy axis is in chain direction with Mn as an exception having the easy axis perpendicular to the chain. The MAE of the chains is in the order of a few meV. We take it as a parameter in the MC calculations.

Some general conclusions can be drawn from Table I. The exchange constants reflect the result that Fe-Fe and Co-Fe wires have a ferromagnetic groundstate in collinear calculations. Antiferromagnetic couplings are present at the beginning of the series. For the freestanding wires, $J_{\text{Fe-Fe}}$ is roughly constant through the series. Cr shows a strong antiferromagnetic intrachain coupling, whereas in V-Fe a strong antiferromagnetic interchain coupling is present. Of course, relaxation effects are reflected in the exchange constants of the embedded systems. The stronger hybridization due to the inward relaxation of the TM chains leads to a decrease of the interchain exchange constants.

TABLE I. Exchange constants for the freestanding TM chain, freestanding TM-Fe wires, and the embedded TM-Fe wires. The definition of the constants in the Heisenberg model incorporates the magnetic spin moments.

J	V (meV)	Cr (meV)	Mn (meV)	Fe (meV)	Co (meV)
Freestanding chain					
$J_{\text{TM-TM}}$	83.87	-155.24	-11.96	106.31	138.37
Freestanding wire					
$J_{\text{TM-TM}}$	-12.96	-115.83	-30.00	80.33	65.16
$J_{\text{TM-Fe}}$	-79.69	-26.12	86.69	150.42	115.48
$J_{\text{Fe-Fe}}$	48.30	77.80	82.40	80.33	54.20
Embedded wire					
$J_{\text{TM-TM}}$	22.30	-69.97	-26.12	79.76	67.37
$J_{\text{TM-Fe}}$	-60.37	17.70	74.34	80.00	68.26
$J_{\text{Fe-Fe}}$	65.07	48.50	58.30	74.58	55.60

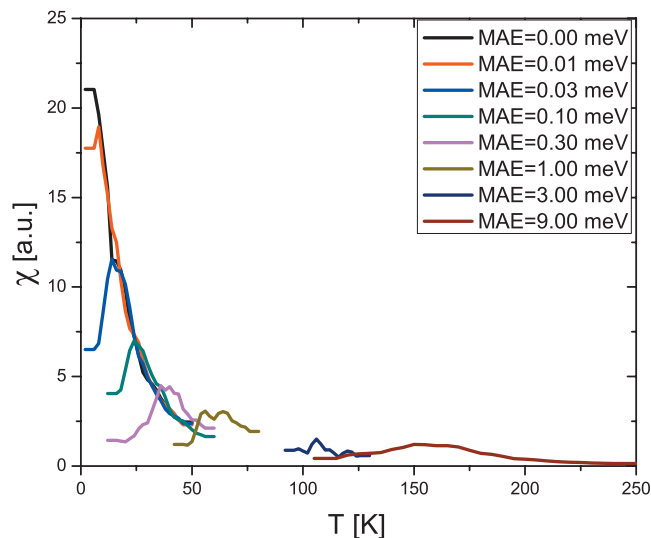


FIG. 3. (Color) Magnetic susceptibility of the embedded Mn–Fe wire for different values of MAE.

Figure 3 shows the susceptibility for an embedded Mn–Fe wire calculated for different MAE values. It can be seen that, in agreement with the Mermin–Wagner theorem,²⁵ there is no magnetic ordering for a vanishing MAE. But for small values, a phase transition can be observed. An increasing anisotropy stabilizes the moments against thermal fluctuation and, thus, leads to an increase of the T_C . Furthermore, the phase transition is broadened. The latter and the relative increase of T_C with respect to the MAE, as shown in Fig. 3, are very similar for the other TMs. All calculated T_C 's are well below room temperature for all systems. A summary of the T_C 's of all systems for MAE=1.00 meV can be found in Table II.

IV. CONCLUSIONS

Ab initio DFT calculations are used to set up Heisenberg models to study finite temperature properties of TM-Fe wires

TABLE II. Critical temperatures for the freestanding and embedded TM-Fe chains for MAE=1.00 meV. The error is approximately $\pm 10\%$.

T_C	V (K)	Cr (K)	Mn (K)	Fe (K)	Co (K)
Freestanding wire	100	20	132	68	75
Embedded wire	88	41	63	122	94

embedded on Cu(111). The critical temperatures of the systems are well below room temperature.

ACKNOWLEDGMENTS

The work is supported by the cluster of excellence Nanostructured Materials of the state Saxony-Anhalt and the International Max Planck Research School for Science and Technology of Nanostructures.

- ¹J. V. Barth, G. Constantini, and K. Kern, *Nature (London)* **437**, 671 (2005).
- ²F. J. Himpsel, J. E. Ortega, G. J. Mankey, and R. F. Willis, *Adv. Phys.* **47**, 511 (1998).
- ³J. Shen, R. Skomski, M. Klaua, H. Jenniches, S. S. Manoharan, and J. Kirschner, *Phys. Rev. B* **56**, 2340 (1997).
- ⁴J. Shen, M. Klaua, P. Ohresser, H. Jenniches, J. Barthel, Ch. V. Mohan, and J. Kirschner, *Phys. Rev. B* **56**, 11134 (1997).
- ⁵J. Guo, Y. Mo, E. Kaxiras, Z. Zhang, and H. H. Weitering, *Phys. Rev. B* **73**, 193405 (2006).
- ⁶C. F. Hirjibehedin, C. P. Lutz, and A. J. Heinrich, *Science* **312**, 1021 (2006).
- ⁷P. Gambardella, A. Dallmeyer, K. Maiti, M. C. Malagoli, W. Eberhardt, K. Kern, and C. Carbone, *Nature (London)* **416**, 301 (2002).
- ⁸Y. Mo, K. Varga, E. Kaxiras, and Z. Zhang, *Phys. Rev. Lett.* **94**, 155503 (2005).
- ⁹S. Lounis, P. H. Dederichs, and St. Blügel, *Phys. Rev. Lett.* **101**, 107204 (2008).
- ¹⁰B. Lazarovits, L. Szunyogh, P. Weinberger, and B. Újfalussy, *Phys. Rev. B* **68**, 024433 (2003).
- ¹¹J. C. Tung and G. Y. Guo, *Phys. Rev. B* **76**, 094413 (2007).
- ¹²C. Ataca, S. Cahangirov, E. Durgun, Y.-R. Jang, and S. Ciraci, *Phys. Rev. B* **77**, 214413 (2008).
- ¹³Y. Mokrousov, G. Bihlmayer, S. Blügel, and S. Heinze, *Phys. Rev. B* **75**, 104413 (2007).
- ¹⁴Y. Mo, W. Zhu, E. Kaxiras, and Z. Zhang, *Phys. Rev. Lett.* **101**, 216101 (2008).
- ¹⁵D. Spišák and J. Hafner, *Phys. Rev. B* **65**, 235405 (2002).
- ¹⁶D. Spišák and J. Hafner, *Phys. Rev. B* **67**, 214416 (2003).
- ¹⁷H. Hashemi, W. Hergert, and V. S. Stepanyuk, *Phys. Rev. B* **81**, 104418 (2010).
- ¹⁸G. Kresse and J. Hafner, *Phys. Rev. B* **48**, 13115 (1993).
- ¹⁹G. Kresse and J. Furthmüller, *Phys. Rev. B* **54**, 11169 (1996).
- ²⁰P. E. Blöchl, *Phys. Rev. B* **50**, 17953 (1994).
- ²¹J. P. Perdew and A. Zunger, *Phys. Rev. B* **23**, 5048 (1981).
- ²²H. Hashemi, W. Hergert, and V. S. Stepanyuk, *J. Magn. Magn. Mater.* **322**, 1296 (2010).
- ²³G. Fischer, M. Däne, A. Ernst, P. Bruno, M. Lüders, Z. Szotek, W. Temmerman, and W. Hergert, *Phys. Rev. B* **80**, 014408 (2009).
- ²⁴A. I. Liechtenstein, M. I. Katsnelson, V. P. Antropov, and V. A. Gubanov, *J. Magn. Magn. Mater.* **67**, 65 (1987).
- ²⁵N. D. Mermin and H. Wagner, *Phys. Rev. Lett.* **17**, 1133 (1966).